

# Simulation of the impacts of climate change on the water budget of the Xitiao River catchment, China

XINGGUO MO & DEJUAN MENG

Key Laboratory of Water Cycle & Related Land Surface Processes, Institute of Geographical Sciences and Natural Resources Research, Chinese Academy of Sciences, Beijing 100101, China  
[moxg@igsnr.ac.cn](mailto:moxg@igsnr.ac.cn)

**Abstract** Climate change has been demonstrated to affect the water budget of a watershed by altering its ecohydrological processes. This study was conducted to quantify water budget changes in Xitiao River catchment from 1960 to 2009 using a distributed ecohydrological process-based model. The result showed that rise of temperature and declines of sunshine duration, air pressure and wind speed were significant, whereas the changes of precipitation and vapour pressure failed a significance test at  $\alpha = 0.05$ . The annual evapotranspiration, precipitation and runoff increased during the last 50 years; however, only the evapotranspiration trend passed the significance test ( $\alpha = 0.05$ ).

**Key words** climate change; ecohydrological process; water budget; VIP model; Xitiao River catchment, China

## 1 INTRODUCTION

Climate change is altering the hydrological cycle processes over the land surface. The impacts of climate change on water budgets cannot be evaluated exactly due to the complicated interacting mechanisms between climate factors, the water cycle and vegetation processes (Wigmosta, 1994). Hydrological dynamic modelling is considered to be an effective approach to understand the forces of the hydrological cycle and reveal its response mechanism to climate change (Krysanova *et al.*, 2005; Holsten *et al.*, 2009; Limousin *et al.*, 2009; Tietje *et al.*, 2010).

The purpose of this paper is to simulate the hydrological process of Xitiao River catchment using a distributed hydrological process-based model (VIP Model) to assess the impacts of climate change on the water budget from 1960 to 2009.

## 2 MODEL DESCRIPTION

The physical process-based model (VIP model), integrated with remotely sensed data, adopted here was first described by Mo *et al.* (2004) for regional ET estimation, in which the canopy and soil surface are treated separately for energy budget and ET estimation. The original model framework is improved with a canopy radiation scheme, as used by Mo & Beven (2004), which distinguishes the leaves spectral properties of visible and near infrared radiation, as well as fraction of direct beam and diffusive radiation.

### 2.1 Evapotranspiration (ET)

ET is calculated as the sum of canopy transpiration ( $E_c$ , mm), interception evaporation ( $E_i$ , mm) and soil evaporation ( $E_s$ , mm).  $E_c$  and  $E_s$  may be estimated with the Penman-Monteith equation considering the wet canopy fraction, expressed as:

$$\lambda E_c = \frac{\Delta R_{nc} + \rho C_p D_0 / r_{ac}}{\Delta + \gamma(1 + r_c / r_{ac})} (1 - W_{fr}) \quad (1)$$

$$\lambda E_s = \frac{\Delta(R_{ns} - G) + \rho C_p D_0 / r_{as}}{\Delta + \gamma(1 + r_s / r_{as})} \quad (2)$$

where  $\Delta$  is the slope of the curve relating saturation water vapour pressure to temperature ( $\text{hPa } ^\circ\text{C}^{-1}$ );  $\gamma$  is the psychrometric constant ( $\text{hPa } ^\circ\text{C}^{-1}$ );  $C_p$  is the specific heat capacity of air ( $\text{J kg}^{-1} ^\circ\text{C}^{-1}$ );  $\rho$  is

the air density ( $\text{kg m}^{-3}$ );  $\lambda$  is the latent heat of vaporization of water ( $\text{J kg}^{-1}$ );  $R_{nc}$  and  $R_{ns}$  are the absorbed net radiation by the canopy and soil surface ( $\text{W m}^{-2}$ ), respectively;  $G$  is the ground heat flux ( $\text{W m}^{-2}$ );  $D_0$  is the saturated vapour deficit at the canopy source (hPa);  $r_c$  is the canopy resistance ( $\text{s m}^{-1}$ );  $r_{ac}$  is the leaf boundary aerodynamic resistance ( $\text{s m}^{-1}$ );  $r_s$  is the soil resistance ( $\text{s m}^{-1}$ );  $r_{as}$  is the soil surface aerodynamic resistance ( $\text{s m}^{-1}$ ); and  $W_{fr}$  is the wet canopy fraction (dimensionless). Vegetation canopy leaf area index (*LAI*) is used to calculate canopy resistances and radiation transfer.

## 2.2 Runoff generation

Surface runoff generation is influenced by soil type, slope and rainfall intensity, and most important control factors to infiltration are precipitation and soil water content, expressed as:

$$Q_s = \frac{P_n^2}{(P_n + \delta)} \quad (3)$$

where  $Q_s$  is surface runoff,  $P_n$  is net precipitation, and  $\delta$  is root zone soil water content deficit (Choudhury, 1998).

## 2.3 Soil water movement

Soil is divided into three layers of thickness 2 cm, 98 cm and 100 cm. The changes of water content in each layer are given by (Sellers *et al.*, 1986):

$$\frac{\partial \theta_1}{\partial t} = \frac{1}{L_1} (P_n - Q_{12} - E_g) \quad (4)$$

$$\frac{\partial \theta_2}{\partial t} = \frac{1}{L_2} (Q_{12} - Q_{23} - E_{tr}) \quad (5)$$

$$\frac{\partial \theta_3}{\partial t} = \frac{1}{L_3} (Q_{23} - Q_3) \quad (6)$$

where  $\theta_i$  is the water content of the  $i$ th soil layer, and  $L_i$  is the thickness of the  $i$ th soil layer.  $Q_{i,i+1}$  ( $i = 1, 2$ ) is the water flux between layers,  $Q_3$  is the deep percolation, set as the gravimetric drainage.

## 2.4 Leaf area index

Remotely sensed information is used for identification of land surface characters, such as the values of fractional vegetation cover and leaf area index. Cover fraction is expressed as the following (Carlson & Ripley, 1997):

$$f_c = \frac{NDVI - NDVI_o}{NDVI_m - NDVI_o} \quad (7)$$

where  $NDVI_o$  and  $NDVI_m$  are the *NDVI* values for bare soil surface and dense canopy, respectively. For relatively homogeneous canopies, there is an approximately exponential relationship between *LAI* and  $f_c$ , expressed as:

$$LAI = -\ln(1 - f_c) / k_{par} \quad (8)$$

where  $k_{par}$  is the canopy extinction coefficient of visible radiation.

## 3 STUDY SITE AND DATA

The Xitiaio River catchment ( $30^{\circ}23' - 31^{\circ}11'N$  and  $119^{\circ}14' - 120^{\circ}29'E$ ) is a branch of the Taihu Lake Basin (Fig. 1). The northern part of the catchment is a plain, and the southern part is a mountainous area. The length of the main stream is 143 km, with a drainage area of 2200  $\text{km}^2$ . The

study area in this paper is the part of the Xitiao River catchment that is located upstream of Gangkou gauge with an area of 1970 km<sup>2</sup>. Annual average precipitation is about 1466 mm with remarkable spatial variation; the annual precipitation may be 300 mm greater in the mountainous area than that on the plain and decreases from southwest to northeast. Annual potential evapotranspiration is 1200 mm, and increases from southwest to northeast.

A data set of seven National Meteorological Observatory (NMO) stations with observations of daily average air temperature, maximum air temperature, minimum air temperature, wind speed, relative humidity, precipitation and sunshine duration for the period 1960–2009 was used. Observed annual discharge data at four hydrological gauges for period 1979–1982, 1984–1986 and 2006–2008 were utilized to validate the model.

GIS and RS data at 250 × 250 m<sup>2</sup> resolution include: (1) bimonthly NDVI data derived from the Terra/Modis product from 2000 to 2009; (2) land use/cover map; (3) a digital elevation model (DEM); and (4) a soil texture map. The 10-year bimonthly NDVI data are averaged to present the seasonal variations of surface characteristics in the study period.

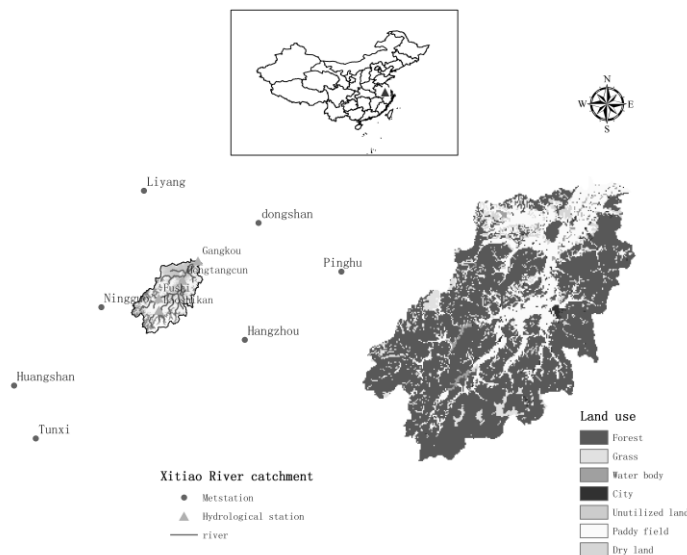


**Fig. 1** DEM and stream (a), land use/cover (b) of the Xitiao River catchment.

## 4 MODEL VALIDATION

Daily climatic values in the seven NMO stations, interpolated by the inverse distance method at 250 m × 250 m grid resolution, were taken as the forcing of the VIP model. NDVI data were used to retrieve LAI as a diagnostic variable of the vegetation condition. Given that long-term change was the focus, runoff was calculated as precipitation minus evapotranspiration, which neglected changes of soil moisture storage. In this study, annual runoff depths of the Xitiao River catchment and its four sub-catchments were employed to validate the VIP model. The agreement between the predicted runoff and observed runoff is favourable with a Pearson correlation coefficient ( $r^2$ ) of 0.64 (Fig. 2).

## 5 RESULTS AND DISCUSSION

### 5.1 Trends of climate factors

Linear trends of air pressure, sunshine duration, air temperature (maximum, minimum, mean), wind speed and vapour pressure were calculated and F tests were applied with a significance level ( $\alpha$ ) of 0.05. Averaged over the whole basin, sunshine duration, wind speed, vapour pressure

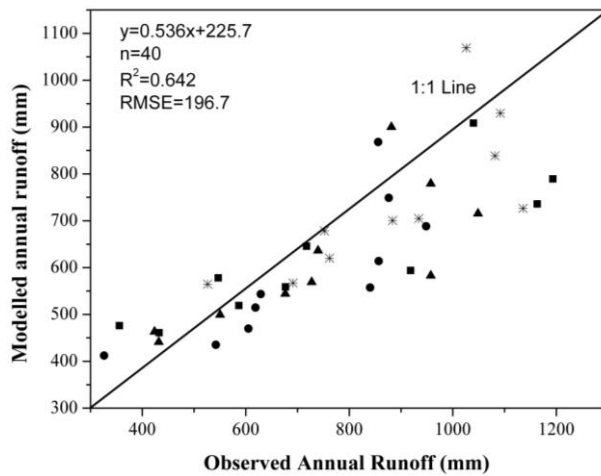


**Fig. 2** Comparison of observed annual runoff with modelled annual runoff simulated by the VIP model (triangle, square, roundness and star represent the value of sub-catchment controlled by the Fushi Reservoir, Hengtangcun, Gangkou and Laoshikan Reservoir stations, respectively).

and air pressure decreased at a rate of  $-0.199$  h,  $-0.104$  m s<sup>-1</sup>,  $-0.001$  kPa and  $-0.646$  hPa per decade, respectively, while mean, maximum and minimum daily temperature increased by  $0.289^{\circ}\text{C}$ ,  $0.279^{\circ}\text{C}$  and  $0.298^{\circ}\text{C}$  per decade. Except for vapour pressure, trends of the other climate factors were significant. In another six river basins and the North China Plain (NCP) in China (the Haihe River, Yellow River, Yangtze River, Huaihe River, Southeast rivers and the Pearl River basins), the change rate range of temperature and wind speed were  $0.12$  to  $0.35^{\circ}\text{C}$  and  $-0.02$  to  $-0.16$  m s<sup>-1</sup> per decade. Compared with those, the declining rate of wind speed in Xitiao River catchment and change rate of mean daily temperature were moderate in China (Liu *et al.*, 2005; Zheng *et al.*, 2009; Cong *et al.*, 2010).

## 5.2 Spatial distribution of water balance

The spatial distributions of the water budget components which were the mean values for 1960–2009 are illustrated in Fig. 3. The spatial pattern of precipitation (P) was closely related with topography, and showed high values in mountainous area in the southern part of the catchment and low values in the downstream plain area in the north of the catchment. The evapotranspiration (ET) was greater in the northern part where paddy fields occupied a very large area. Since runoff was calculated according to precipitation and ET, its spatial distribution was more complex. Figure 3(c) shows that the runoff (R) was larger in the mountainous area than in the plain and the paddy fields. Soil moisture (SW) in Fig. 3(d) shows higher values in the paddy field and the main stream valley than other areas. In the northern mountainous area, soil moisture was higher than elsewhere, resulting from the higher precipitation there.

## 5.3 Temporal variation of water budget

The water budget will change with the variation of climate factors and vegetation processes, and at the same time the water budget and climate will affect vegetation growth and distribution. The variations of the water budget from 1960 to 2009 for the whole catchment and in different land-use types are shown in Fig. 4 and Table 1 to represent the effects of climate change. The water budgets fluctuated corresponding to the inter-annual climate variability during the last 50 years, in which precipitation, ET and runoff increased; however, only the ET trend passed the significance test ( $\alpha = 0.05$ ). Trends of actual ET in forest and grass areas were more obvious than for other land-cover types. Attribution analysis was used to analyse the reason for the significant increasing trend of ET. Using the attribution method presented by Roderick *et al.* (2007), wind speed made the

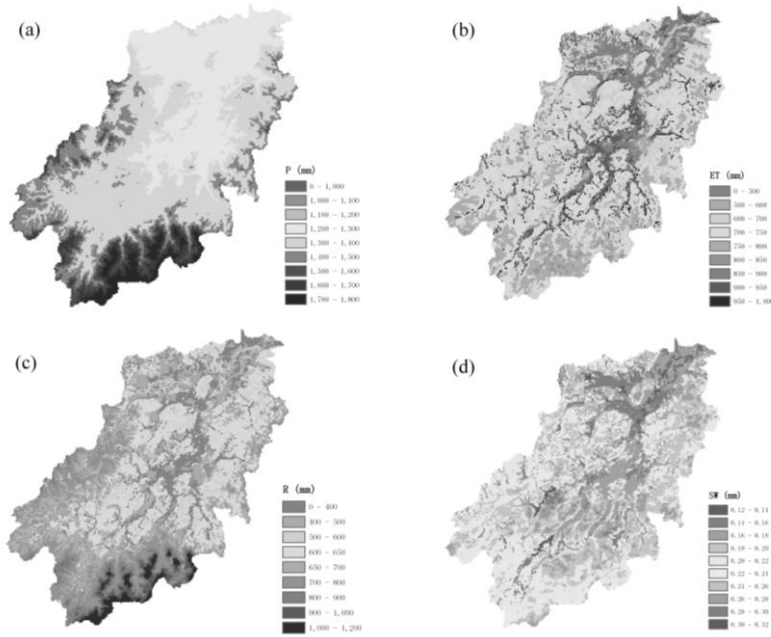


**Fig. 3** Spatial distribution of water budget: (a) precipitation; (b) evapotranspiration; (c) runoff; and (d) soil moisture in Xitiao River catchment.

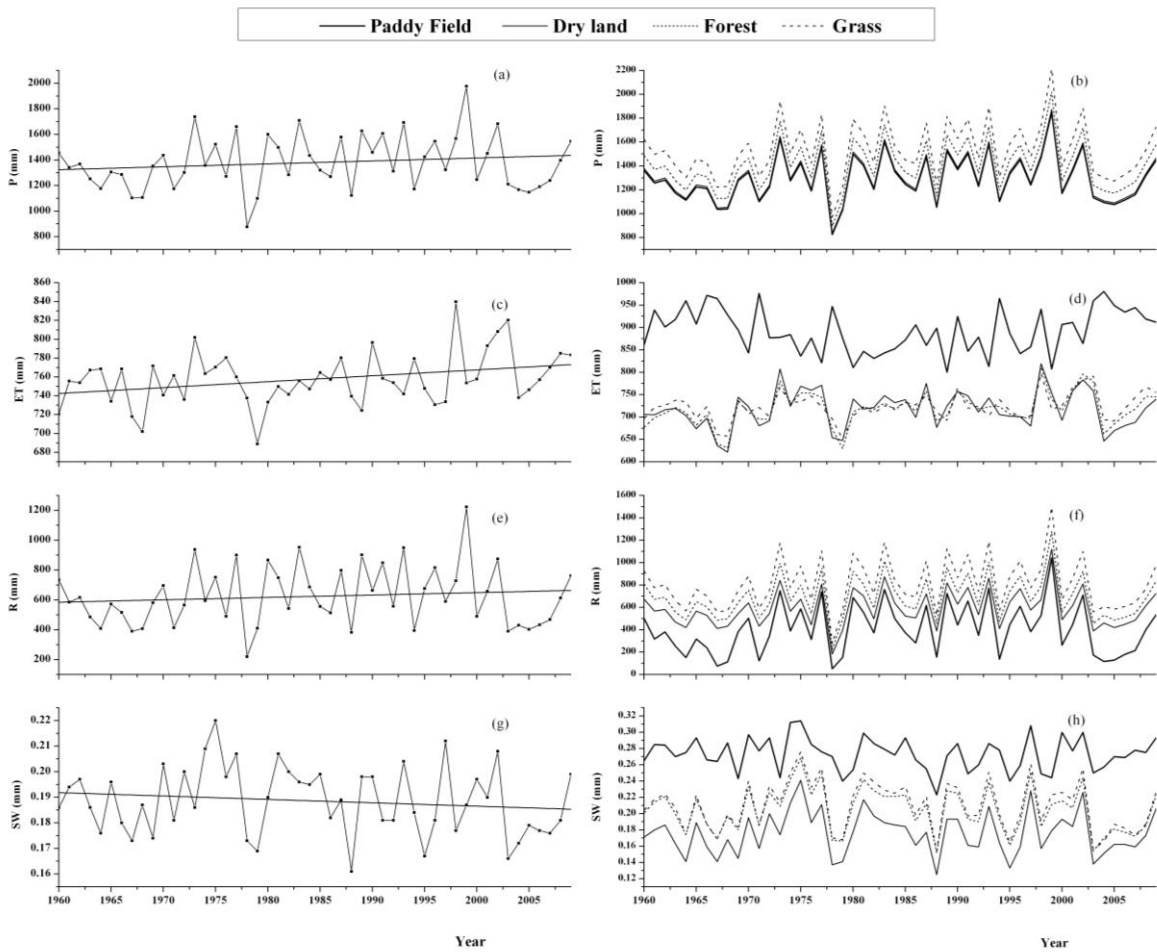


**Fig. 4** Temporal variations of water budget (left panel for whole catchment; right panel for different land-cover types).

**Table 1** Linear trends of water budget (mm/year).

	Mean	Paddy field	Dry land	Forest	Grass
P	2.292	2.101	2.139	2.357	2.630
ET	0.627*	0.059	0.408	0.839*	0.692*
R	1.609	1.929	1.730	1.518	1.939
SW	-0.000	-0.000	0.000	-0.000	-0.000

\* means significant change.

greatest contribution ( $-3.0 \text{ mm year}^{-1}$ ) to potential evapotranspiration ( $ET_p$ ), followed by temperature ( $1.1 \text{ mm year}^{-1}$ ), sunshine duration ( $-0.9 \text{ mm year}^{-1}$ ) and vapour pressure ( $0.5 \text{ mm year}^{-1}$ ), and the integrated action of the four factors lead to decreasing  $ET_p$ . However, ET was influenced not only by  $ET_p$ , but also precipitation. Thus, multiple linear regression was studied between ET and climate factors (temperature, vapour pressure, sunshine duration, wind speed and precipitation). The results showed that the standardized coefficient were ranked as temperature (0.374), precipitation (0.315), vapour pressure (0.237), sunshine duration (0.076) and wind speed ( $-0.031$ ), and the trends of first three factors made positive influence to the increase of ET.

Temporal variations of water budgets with different land use types are shown in Fig. 4(b), (d), (f), (h). There was almost no difference between precipitation on paddy field and dry land, whereas grassland precipitation and precipitation in forest were greater. The reason is that the mountains and upstream areas with more precipitation are where the grass and forest are located. ET in paddy field was much greater than for other land-cover types whose annual ET amounts were quite similar to each other. However, runoff values in the four cover areas were different and paddy field showed the poorest capacity to generate runoff due to the smaller difference between precipitation and evapotranspiration there. The soil profile in dry land held the smallest water storage and paddy field held the largest, while soil moisture values in forest and grassland were similar. Across the areas of the four land cover types, temporal variations of precipitation, runoff and soil moisture were similar during the last 50 years. Compared with the other three type areas, ET in paddy field areas showed different temporal variations. This is interpreted as due to the main limiting factor for ET in paddy fields is atmospheric water demand (energy); whereas, for the other land use types, the main ET limiting factor is water availability.

## 6 CONCLUSION

This paper quantified the impacts of climate change on the water budget in Xitiao River catchment using a distributed ecohydrological process-based model (VIP Model). The result showed that rise of temperature and declines of sunshine duration, air pressure and wind speed were significant (with a significance level of 0.05) from 1960 to 2009, whereas the change of vapour pressure failed the significance test. ET, precipitation and runoff increased during the last 50 years, but only the trend of ET passed the 0.05 significance test.

## REFERENCE

- Carlson, T. N. & Ripley, A. J. (1997) On the relationship between fractional vegetation cover, leaf area index and NDVI. *Remote Sens. Environ.* **62**, 241–252.
- Choudhury, B. J. (1998) A biophysical process-based estimate of global land surface evaporation using satellite and ancillary data (I): Model description and comparison with observations. *J. Hydrol.* **205**, 164–185.
- Cong, Z. T., Zhao, J. J., Yang, D. W. & Ni, G.H. (2010) Understanding the hydrological trends of river basins in China. *J. Hydrol.* **388**, 350–356.
- Holsten, A., Vetter, T. & Vohland, K., (2009) Impact of climate change on soil moisture dynamics in Brandenburg with a focus on nature conservation areas. *Ecol. Model.* **220**(17), 2076–2087.
- Krysanova, V., Hattermann, F. & Wechsung, F. (2005) Development of the ecohydrological model SWIM for regional impact studies and vulnerability assessment. *Hydrol. Processes* **19**, 763–783, doi:10.1002/hyp.5619.

- Ivanov, V. Y., Bras, R. L. & Vivoni, E. R. (2008) Vegetation–hydrology dynamics in complex terrain of semiarid areas: 1. A mechanistic approach to modeling dynamic feedbacks. *Water Resour. Res.* **44**, W03429, doi:10.1029/2006WR005588.
- Limousin, J. M., Rambal, S. & Ourcival, J. M. (2009) Long-term transpiration change with rainfall decline in a Mediterranean *Quercus ilex* forest. *Global Change Biol.* **15**(9), 2163–2175.
- Liu, S., Qiu, J. & Mo, X. (2009) Wind velocity variation from 1951 to 2006 in the North China Plain. *Resour. Sci.* **31**(9), 1486–1492 (in Chinese with English abstract).
- Mo, X. & Beven, K. (2004) Multi-objective conditioning of a three-source canopy model for estimation of parameter sensitivity and prediction uncertainty. *Agric. For. Met.* **122**, 39–63.
- Mo, X., Liu, S., Lin, Z. & Zhao, W. (2004) Simulation the spatial and temporal variation of evapotranspiration in the Lushi Catchment. *J. Hydrol.* **285**, 125–142.
- Roderick, M. L., Rotstayn, L. D., Farquhar, G. D. & Hobbins, M. T. (2007) On the attribution of changing pan evaporation. *Geophys. Res. Lett.* **34**, L17403, doi:10.1029/2007GL031166.
- Sellers, P. J., Mintz, Y., Sud, Y. C. & Dalcher A. (1986) A simple biosphere model (SiB) for use within general circulation models. *J. Atmos. Sci.* **43**, 305–331.
- Tietjen, B., Jeltsch, F., Zehe, E., Classen, N., Groengroeft, A., Schifffers, K. & Oldeland, J. (2010) Effects of climate change on the coupled dynamics of water and vegetation in drylands. *Ecohydrol.* **3**(2), 226–237.
- Wigmosta, M.S., Vail Lance, W. & Lettenmaier, D. P. (1994) A distributed hydrology–vegetation model for complex terrain. *Water Resour. Res.* **30**(6), 1665–1679.
- Zheng, H. X., Liu, X. M., Liu, C. M., Dai, X. Q. & Zhu, R. R. (2009) Assessing contributions to pan evaporation trends in Haihe River Basin, China. *J. Geophys. Res.* **114**, D24105, doi:10.1029/2009JD012203.